ELSEVIER

Polymer 44 (2003) 1697–1703

polymer

www.elsevier.com/locate/polymer

Microstructural development of a vitrified hindered phenol compound during thermal annealing

Chifei Wu*

Institute of Material Science and Technology, East China University of Science and Technology, 130 Meilong-lu, Shanghai 200237, People's Republic of China

Received 29 March 2002; received in revised form 18 November 2002; accepted 28 November 2002

Abstract

Structural changes in vitrified 3,9-bis{1,1-dimethyl-2[β-(3-*tert*-butyl-4-hydroxy-5-methylphenyl)propionyloxy]ethyl}-2,4,8,10-tetraoxaspiro[5,5]-undecane (AO-80) during the annealing process were studied by DSC, WAXD and FT-IR. The initial AO-80 is highly crystalline, whereas AO-80 obtained by cooling from its melting state is an amorphous material. Annealing treatments below the melting point of AO-80 resulted in structural development. In addition, the modification of the crystal formed by annealing treatment depended on the annealing conditions. The IR spectra of various crystal modifications were different. Analysis of the microstructures of the crystals that formed indicated that the crystal formed by annealing at 100 °C is a smectic crystal, whereas the crystal formed by annealing at 80 °C is a nematic crystal. The AO-80 crystal formed within the chlorinated polyethylene (CPE) matrix during annealing at 100 °C is also a nematic crystal. Though the CPE matrix decreased regularity of AO-80 crystals, it raised the growth rate of AO-80 crystals.

Keywords: Hindered Phenol; Chlorinated polyethylene; Fourier transform infrared spectra

1. Introduction

Polymers are often mixed with characteristic low-molecular-weight compounds to improve their properties and to discover useful unknown functions. The properties and structures of matrix polymers have been investigated extensively, whereas little attention has been paid to the low-molecular-weight compound additive. Hindered phenol compounds such as 3,9-bis{1,1-dimethyl-2[β-(3-*tert*-butyl-4-hydroxy-5-methylphenyl)propionyloxy]ethyl}-2,4,8,10-tetraoxaspiro[5,5]-undecane, which is abbreviated as AO-80, are commonly used as antioxidants of polymers [1]. In addition, AO-80 has recently been found to be an additive with multiple functions [2–4]. The addition of AO-80 into some polarized polymer such as chlorinated polyethylene (CPE) can greatly improve their damping properties [5]. On the other hand, reversible hydrogen bonding between CPE and AO-80, which acts as the tie points for the CPE-rich continuous phase, can lead to the evolution of shape memory function [6]. In addition, the addition of AO-80 into an incompatible acrylate rubber/chlorinated polypropylene blend can cause not only a remarkable enhancement of compatibility but also the grant of very large peel strength [7]. In these cases, the effectiveness of the additive was found to depend not only on the chemical nature and content of the additive but also on its molecular aggregation state [8–11]. It is well known that most of the antioxidants are polymorphous materials form different physical structures below their melting points (glassy state or different crystal modifications) [12–15]. Consequently, full knowledge of the aggregation state is desirable if optimum material performance is required.

In another study of this series [16], structural change in vitrified AO-80 during annealing at 100 °C was investigated. Vitrified AO-80 that was annealed at 100 °C showed an endothermic peak just above its glass-transition temperature. This endothermic peak was assigned to a primary transition from an ordered state formed during annealing to a disordered state. In the case of vitrified AO-80 annealed at 100 °C for 74 h, the ordered structure organized by one intermolecular hydrogen bonds was substantiated by the existence of a peak at 21.5° in wide-angle X-ray diffraction trace. Our attention has been limited to the origin of this

* Tel./fax: +86-21-64252569.
E-mail address: wucf@ecust.edu.cn (C. F. Wu).

0032-3861/03/$ - see front matter © 2003 Elsevier Science Ltd. All rights reserved.
doi:10.1016/S0032-3861(02)00918-7

endothermic peak at that time. However, crystallization of AO-80 from its amorphous state during a longer time of annealing has not been studied. In this study, we examined in detail the formation and development of an AO-80 crystal from an amorphous state during a long time of annealing at a temperature below the melting point of AO-80.

2. Experimental

2.1. Materials

The AO-80 (as shown in Fig. 1) is a commercial antioxidant (ADK STAB AO-80, Asahi Denka Industries Co., Japan). The initial AO-80 is highly crystalline, whereas AO-80 obtained by cooling from its melting state is amorphous. The glass-transition temperature of amorphous AO-80 is 41 °C, and the melting point and melting enthalpy of crystalline AO-80 are 119 °C and 97 J g^{-1}, respectively. For annealing, the vitrified AO-80 particles were placed in a constant temperature chamber at 100 °C which is lower than the melting point of AO-80 for appointed time and then were quenched into an ice-water bath.

To examine the crystal formation and its development of amorphous AO-80 dispersed within CPE matrix, the blends of CPE and vitrified AO-80 were also prepared. The CPE used as a matrix in this study was described in a previous paper [10]. The AO-80 content was 40 wt% for all samples. The CPE was first kneaded by a mixing roller for 5 min, then the particles of vitrified AO-80 were added to the kneaded CPE and the mixture was kneaded at room temperature for 10 min. Moreover, the kneaded specimens were placed in a constant temperature chamber at 100 °C for various times and then quenched into an ice-water bath.

2.2. Differential scanning calorimetry

In order to determine the effects of annealing on thermal behavior of AO-80, differential scanning calorimetry (DSC) (Shimadzu TA-50WS) measurements were carried out. Samples of about 5 mg in weight and sealed in an aluminum pan were heated from − 100 to 160 °C at a scanning rate of 10 °C min^{-1} under a nitrogen atmosphere.

2.3. Wide-angle X-ray diffraction

The structural change of the vitrified AO-80 during annealing was confirmed by wide-angle X-ray diffraction (WAXD) (RIKAKU RU-200) measurement. While for vitrified AO-80 the sheets with a thickness of about 1 mm were prepared, for crystalline AO-80 its powders were sealed in polyethylene films with a thickness of about 50 μm. The Cu Kα radiation (50 kV, 180 mA, $\lambda = 0.15418$ nm) monochromatized with a Ni-filter was used, and intensity data were obtained with a scintillation counter. The diffraction intensity profile at the detector was treated according to pin hole geometry.

2.4. Fourier transform infrared spectra (FT-IR)

IR spectra were obtained with a JEOL JIR-100 spectrometer. The spectra of AO-80 were taken at ambient temperature in KBr. The scanned wavenumber range was 4000–400 cm^{-1}. All the measurements were carried out at a resolution of 2 cm^{-1} and scan times of 100.

3. Results and discussion

3.1. Melting behavior of vitrified AO-80 that has been annealed

The thermal properties of vitrified AO-80 annealed at 100 °C are shown in Fig. 2 and Table 1. While the initial AO-80 showed a very large melting peak with a maximum at 119 °C and $\Delta H = 97$ J g^{-1}, vitrified AO-80 showed a second-order transition at 42 °C. It was found that heat treatment at 100 °C caused a change from an amorphous state to a crystalline state. With an increase in annealing time (up to 134 h), the specific heat of the second-order transition at 42 °C decreased, whereas two other melting peaks increased. The temperature positions of the two melting peaks are notable. The higher melting peak is higher than the melting point (T_m) of initial AO-80, whereas the lower melting peak is lower than T_m. The results suggest that AO-80 exhibits at least three solid phases (polymorphs). With a further increase in annealing time up to 153 h, the lower melting peak became a smaller shoulder, but the higher melting peak increased and its peak location shifted to a higher temperature, suggesting that there is a structural transformation from a relatively unstable crystal to a more stable crystal during annealing (134–153 h). When the annealing time was further increased, the higher melting peak became high and sharp. A comparison of the melting enthalpy of vitrified AO-80 annealed at 100 °C for 588 h (68 J g^{-1}) and that of the initial AO-80 (97 J g^{-1}) showed that the crystallization of AO-80 from an amorphous state at 100 °C is incomplete even after 588 h. In summary, the

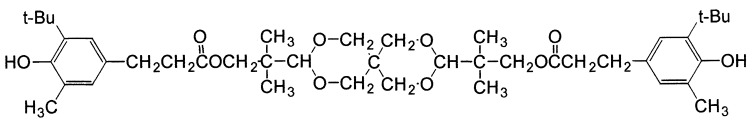

Fig. 1. Chemical structure of 3,9-bis{1,1-dimethyl-2[β-(3-*tert*-butyl-4-hydroxy-5-methylphenyl)propionyloxy]ethyl}-2,4,8,10-tetraoxaspiro[5,5]-undecane, which is abbreviated as AO-80.

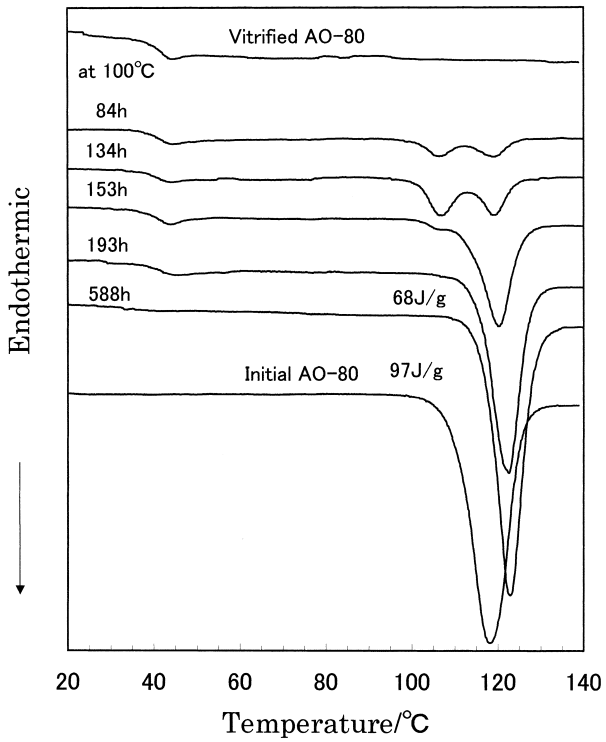

Fig. 2. DSC curves of vitrified AO-80, initial AO-80, and vitrified AO-80 annealed at 100 °C.

process in annealing treatment for 588 h can be classified into four regimes: (1) formation of an ordered intermediate structure (~74 h) [16], (2) growth of two kinds of crystals (74–134 h), (3) transition from a relatively unstable crystal to another more stable crystal (134–193 h) and (4) further growth of a highly stable crystal (~193 h).

In order to determine the effects of annealing temperature, annealing treatment of vitrified AO-80 at 80 °C was also carried out. Fig. 3 shows the change in thermal behavior of vitrified AO-80 as a function of annealing time. The sample annealed at 80 °C for 50 h showed a small endothermic peak just above the glass-transition temperature, a shoulder and a large endothermic (melting) peak. This melting characteristic implies that AO-80 in this case is a medley of several elements containing glass, paracrystal (shoulder) and crystals (large endothermic peak). The tendency of the change in DSC curves caused by more prolonged annealing is similar to that in the case of

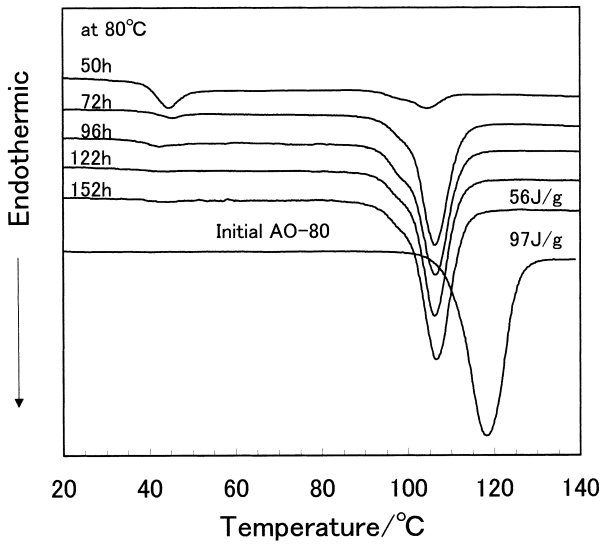

Fig. 3. DSC curves of vitrified AO-80, initial AO-80, and vitrified AO-80 annealed at 100 °C.

annealing at 100 °C. However, the T_m of the crystal formed at 80 °C is lower. This result suggests that AO-80 has many crystalline modifications.

3.2. Confirmation of polymorphism by WAXD

WAXD patterns were recorded to confirm the existence of many crystalline modifications. Fig. 4 shows the X-ray diffraction traces of various annealed samples. It was found that the diffraction profiles of the initial AO-80, vitrified AO-80 that were annealed at 80 and 100 °C are different. The initial AO-80, which was cultured from a dilute solution, showed many stronger diffraction peaks, and the trace consisting of them is a typical diffraction profile of a crystal of a low-molecular-weight compound. In the case of vitrified AO-80 annealed at 100 °C for 134 h, the diffraction profile was slightly different from those of samples annealed for 153 and 588 h, supporting the speculation that the crystalline modifications corresponding to the two melting peaks (108 and 120 °C) shown in Fig. 2 are different. In addition, the diffraction profile of vitrified AO-80 annealed at 80 °C was not the same as that of vitrified AO-80 annealed at 100 °C or the same as that of initial AO-80.

Table 1
Glass–transition temperature (T_g), melting point (T_m) and enthalpy of fusion (ΔH_m) corresponding to the DSC thermograms in Figure 2

		T_g(°C)	T_{m1}(°C)	ΔH_{m1}(Jg^{-1})	T_{m2}(°C)	ΔH_{m1}(Jg^{-1})
Initial AO–80		/	/	/	119	97
Vitrified AO–80		42	/	/	/	/
Vitrified AO–80 annealed at 100 °C	84 h	42	106	4	119	5
	134 h	42	106	10	119	9
	153 h	42	106	2	120	28
	193 h	42	/	/	121	52
	588 h	/	/	/	123	68

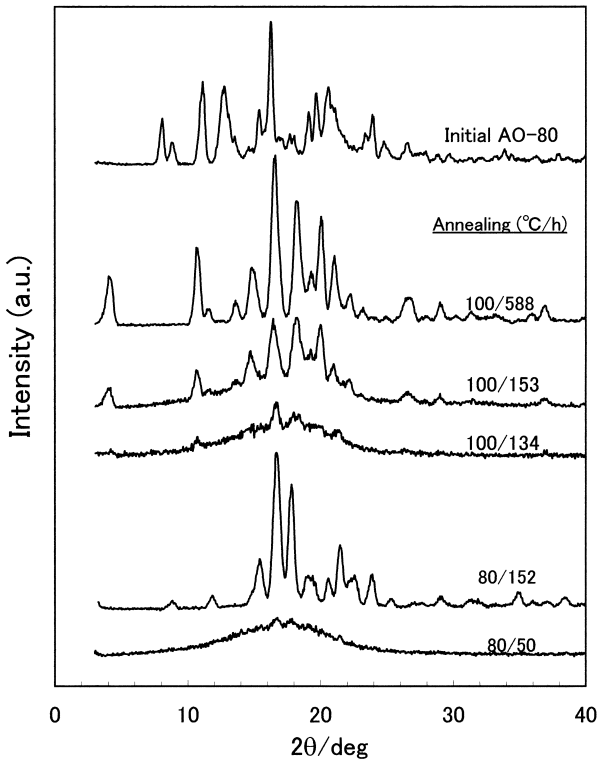

Fig. 4. Wide-angle X-ray diffraction traces of initial AO-80 and vitrified AO-80 annealed at 100 °C.

Thus, these different diffraction profile indicate that AO-80 is a polymorphous material.

From Fig. 4, another intriguing observation is that there is a diffraction peak at $2\theta = 4.15°$ (corresponding to 4.26 nm of layer interval) for vitrified AO-80 annealed at 100 °C for 153 and 588 h. It is well known that a stronger diffraction peak in a smaller range of angles is observable in the case of smectic crystal, and that it corresponds to the length of the molecule. Therefore, the crystal formed by annealing at 100 °C for a longer time may be a smectic crystal. On the other hand, in the cases of vitrified AO-80 annealed at 80 °C, a stronger diffraction peak in a smaller range of angles was not observed. This implies that the crystal formed by annealing at 80 °C may be a nematic crystal.

3.3. Difference in IR spectra due to crystalline polymorphism

A change in the intermolecular interaction on annealing processes is also of interest because the crystallization of AO-80 resulting from annealing treatment must induce the recombination of intermolecular hydrogen bonding. FT-IR spectroscopy is a quite suitable technique for investigating the specific intermolecular interactions. Fig. 5 shows the IR spectra of the initial and vitrified AO-80 in the ranges of 3800–3200 and 1800–1500 cm^{-1}. It is obvious that there are differences in the strengths and positions of IR absorption peaks resulting from the carbonyl group

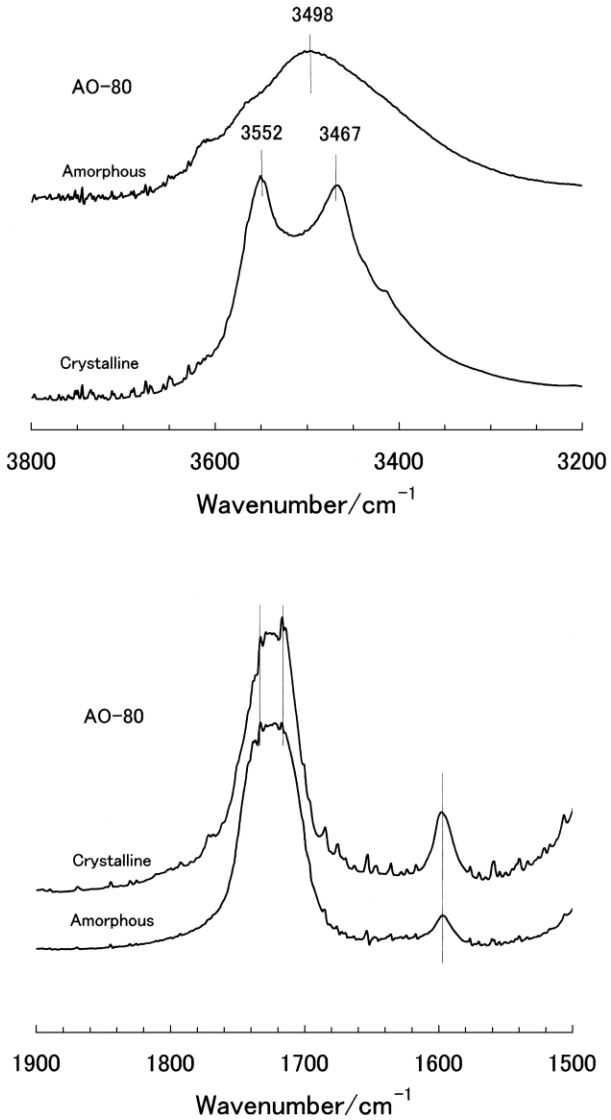

Fig. 5. Scale-expanded infrared spectra of the initial and vitrified AO-80 recorded at room temperature in the ranges of 3800–3200 (a) and 1800–1500 cm^{-1} (b).

(C═O) and hydroxyl group (OH). However, interpretation of those bands is troublesome.

Analysis of the FT-IR spectra confirmed qualitatively that intermolecular hydrogen bonds are formed between C═O and OH (or π-electrons). Fig. 6 shows an illustration of the experimental and fitted spectra of amorphous AO-80 in the C═O vibration region. As can be seen in the figure, a complex band profile corresponding to the stretching vibration of the carbonyl group (C═O) of amorphous AO-80 was divided into three distinct absorption bands. The good agreement between experimental and fitted spectra indicates the reliability of this fitting. The band at 1738 cm^{-1} is assigned to 'free' C═O (monomer), whereas the band at 1712 cm^{-1} is related to hydrogen bonding between C═O and OH. As shown by Pimentel et al. [17], the shift observed for the stretching vibration can be roughly related to the O–H···O distance. The frequency of the

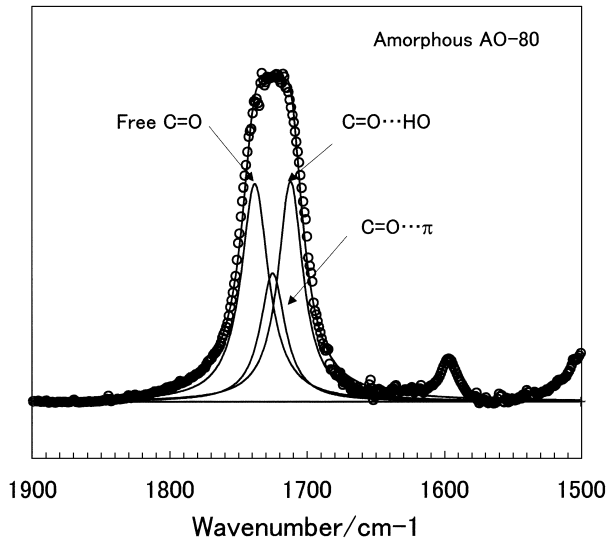

Fig. 6. Experimental and fitted spectra for vitrified AO-80 in the carbonyl vibration region. Expt.: experimental spectrum; Fitt.: fitted spectrum, the sum of the free C═O component and hydrogen bonds (C═O···HO and C═O···π-electrons) component.

stretching IR band of both crystalline and amorphous AO-80, thus, gives a rough estimate of the order degree of AO-80 molecules. Therefore, the band at 1725 cm^{-1} is probably related to hydrogen bonding between C═O and π-electrons.

For crystalline AO-80, the band observed at 3552 cm^{-1} is assigned to an intermolecular hydrogen bond between OH and C═O, whereas the band at 3468 cm^{-1} is assigned to self-assembly of OH. A comparison of the shape of spectra corresponding to the stretching vibration of C═O of crystalline and amorphous AO-80 indicates that there are few free C═O groups, but there are many hydrogen-bonded C═O groups in crystalline AO-80. This implies that there are two types of hydrogen-bonded C═O (C═O···OH and C═O···π-electrons) in addition to self-assembly of OH for crystalline AO-80. In addition, a X-ray diffraction peak in a smaller range of angles corresponding to the length of straightened AO-80 was not observed. These results suggest that crystals of initial AO-80 are a nematic form. On the other hand, in the case of amorphous AO-80, the two bands at 3552 and 3467 cm^{-1} disappeared, but another broader band clearly appeared at 3498 cm^{-1}. The appearance of the broader band implies that there may be many intermolecular interactions.

Fig. 7 shows IR spectra of the vitrified AO-80 heat-treated at 100 °C in the ranges of 3800–3200 and 1800–1500 cm^{-1}. For the heat-treated samples, with an increase in annealing time (up to 134 h), there was almost no change in the shape of the band corresponding to the stretching vibration of C═O compared to that of untreated AO-80. However, a comparison of Figs. 6 and 7 indicates that with a further increase in annealing time, a band due to free C═O (1738 cm^{-1}) increases, whereas another band due to hydrogen-bonded C═O (1712 cm^{-1}) decreases. In particular, in the sample that was annealed at 100 °C for 588 h, most of the C═O groups are free.

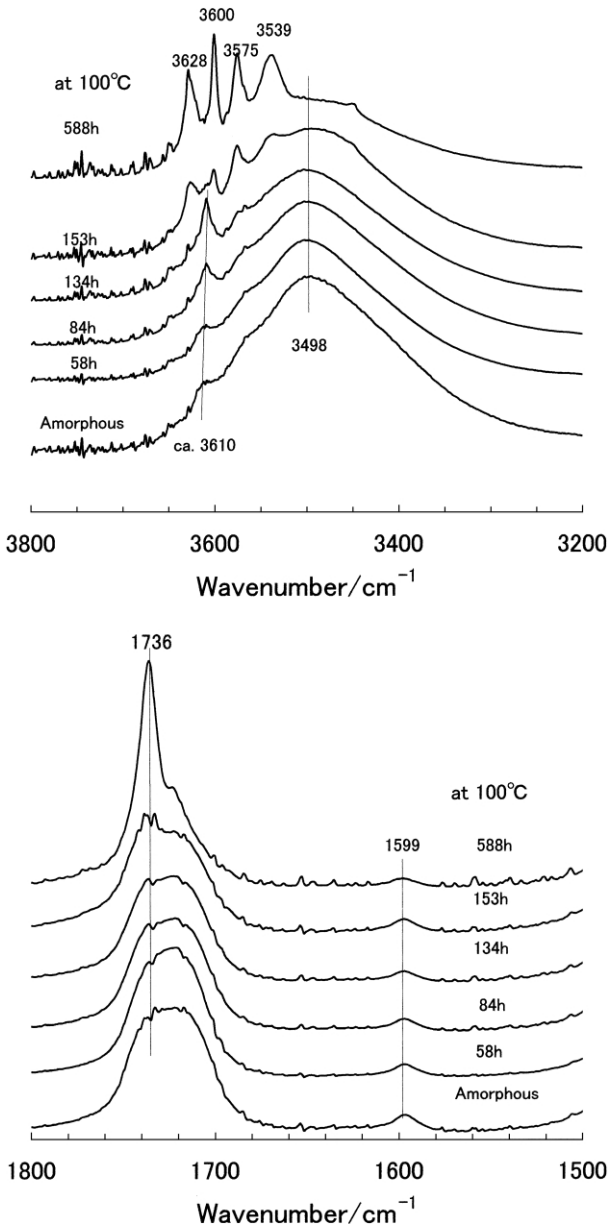

Fig. 7. Scale-expanded infrared spectra of vitrified AO-80 annealed at 100 °C recorded at room temperature in the ranges of 3800–3200 (a) and 1800–1500 cm^{-1} (b).

In addition, the changes in another absorption corresponding to the stretching vibration of OH are also of interest. A band about 3610 cm^{-1}, which may be assigned to C═O···π-electron, increased with an increase in annealing time (up to 134 h). However, with a further increase in annealing time, this band disappeared, but four other bands clearly appeared at 3539, 3575, 3600, and 3628 cm^{-1}. These results also support the speculation that the crystalline modifications corresponding to the two melting peaks shown in Fig. 2 are different.

A comparison of the spectra of crystalline AO-80 in

the range of 3800–3200 showed that the ν_{OH} frequency (3539, 3575, 3600, and 3628 cm^{-1}) of vitrified AO-80 annealed at 100 °C for 588 h is lower than that (3552 and 3467 cm^{-1}) of initial AO-80 (highly crystalline). This implies that the bond strength of the former is smaller than that of the latter.

In addition, we believe that four bands (at 3539, 3575, 3600, and 3628 cm^{-1}) shown in Fig. 7 are assigned to self-assembly of OH, hydrogen bonds (OH···π-electrons and C═O···π-electrons), and free OH, respectively. Assuming that all AO-80 molecules are represented as 'bent bar', the length from one OH to another OH is about 2.7 nm. If all ends of AO-80 molecules are arranged in two planes, its layer interval should be 2.7 nm of molecular length. This value is smaller than the observed value (4.26 nm). The discrepancy is due to the existence of some hydrogen bonds, such as OH···π-electrons and C═O···π-electrons, in addition to self-assembled OH.

Fig. 8 shows IR spectra of vitrified AO-80 heat-treated at 80 °C in the ranges of 3800–3200 and 1800–1500 cm^{-1}. With an increase in annealing time, the shape of the absorption band due to C═O became sharper than that of untreated AO-80, implying that the hydrogen bond between C═O and π-electrons increase in number, whereas free C═O and the hydrogen bond between C═O and OH decreases. In addition, two bands, particularly the band at 3608 cm^{-1}, which is assigned to an intermolecular hydrogen bond between C═O and π-electrons, became larger. Deliberating on the results of DSC, WAXD and FT-IR, the crystal formed by annealing at 80 °C can be considered to also be a nematic crystal, but its regularity may be lower than that of initial AO-80.

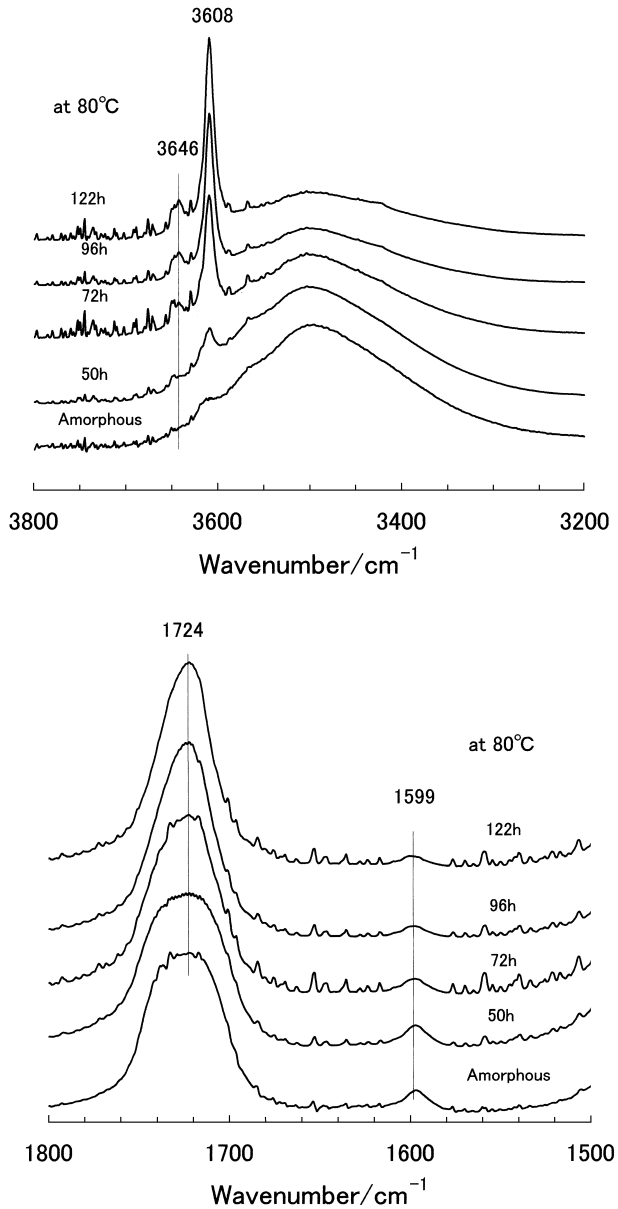

Fig. 8. Scale-expanded infrared spectra of vitrified AO-80 annealed at 80 °C recorded at room temperature in the ranges of 3800–3200 (a) and 1800–1500 cm^{-1} (b).

3.4. Crystallization of vitrified AO-80 within CPE matrix during annealing

The microstructural development of amorphous AO-80 dispersed within CPE matrix during annealing process is also important. Fig. 9 shows the change in melting behavior of CPE/vitrified AO-80 as a function of annealing time. It was found that annealing treatment at 100 °C caused a change in the aggregation state of AO-80 molecules within the CPE matrix. With an increase in annealing time (up to 60 min), the melting peak near 100 °C increased in association with a decrease in a jump near 40 °C due to the glass-transition of amorphous AO-80. When the annealing time was increased to more than 120 min, the jump due to glass-transition of amorphous AO-80 disappeared, and the increase in the melting peak of AO-80

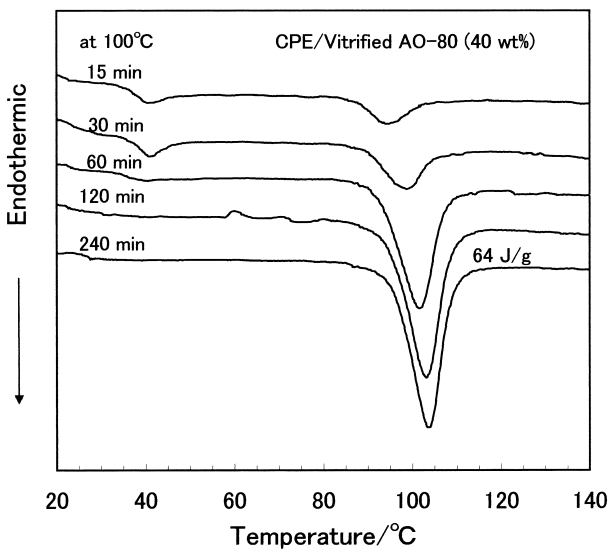

Fig. 9. DSC curves of CPE/vitrified AO-80 (40 wt%) annealed at 100 °C for different annealing times (min). Scan rate was 10 °C min^{-1}.

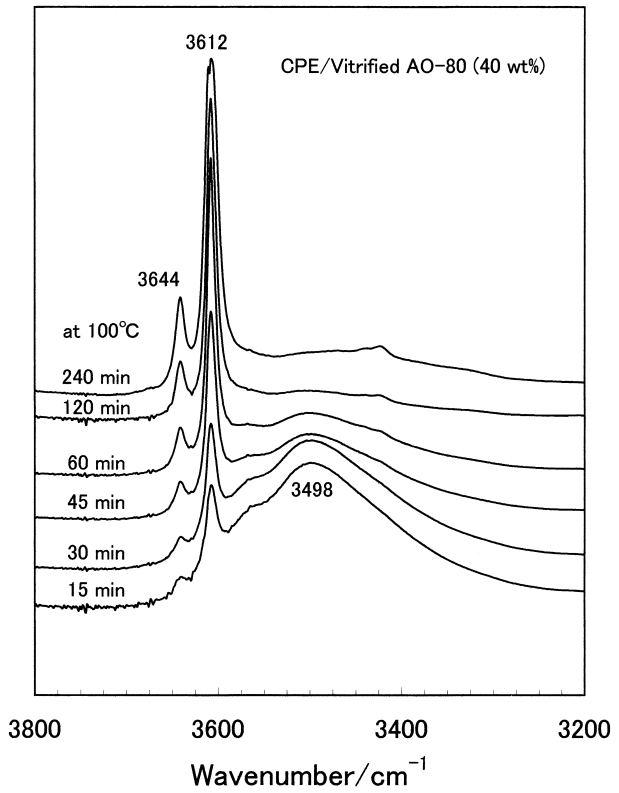

Fig. 10. IR spectra (in the hydroxyl-stretching region) of the vitrified AO-80 within CPE annealed at 100 °C for different annealing times (min).

crystals stopped. This tendency is similar to that in the case of annealing at 80 °C for pure amorphous AO-80. This result suggests that the AO-80 crystal formed within the CPE matrix during annealing at 100 °C may also be a nematic crystal. This proposition will be further substantiated by the results of anaiysis of IR spectra.

Fig. 10 shows IR spectra centered near 3500 cm^{-1} corresponding to OH groups for various annealing CPE/vitrified AO-80 samples. With an increase in annealing time, the band at 3498 cm^{-1} gradually become low, whereas two new bands appeared at 3644 and 3612 cm^{-1}. This result agrees with the change in infrared spectra of amorphous AO-80 during annealing at 80 °C.

A comparison of pure amorphous AO-80 and amorphous AO-80 within CPE matrix at same annealing temperature showed that the existence of polymer chain largely influences the formation and development of AO-80 crystals. At same annealing temperature (100 °C), the crystal obtained from pure amorphous AO-80 is a smectic crystal, whereas the crystal formed within the CPE matrix is a nematic crystal. The fall of melting temperature of the AO-80 crystal that formed within the CPE matrix can be accounted for by the decrease in the regularity due to the incorporation of some chains of CPE within an AO-80 crystal. On the other hand, with an increase in annealing time, the melting temperature of the crystal formed at 80 °C from pure amorphous AO-80 hardly changes (Fig. 3), whereas that of the crystal formed within the CPE matrix greatly increases (Fig. 9). This difference implies that the CPE chain that was incorporated into the AO-80 crystal was continuously eliminated with an increase in annealing time.

In contrast, the difference in the growth rate of the AO-80 crystals should also be noted. The rate growth of the AO-80 crystal crystals for CPE/vitrified AO-80 is larger than that of pure amorphous AO-80 annealed at either 100 or 80 °C. Though regularity of the AO-80 crystals decreased, the growth rate of AO-80 crystals was raised by the existence of the CPE chains. This is an intriguing phenomenon; further discussion will be presented in a later paper.

4. Conclusions

Thermal melting properties of vitrified AO-80 during annealing at 80 and 100 °C were investigated. The initial AO-80 is highly crystalline, whereas AO-80 obtained by cooling from its melting state is amorphous. DSC measurements revealed that there is a structural development of vitrified AO-80 during the annealing process. In addition, the form of the crystal formed depends on annealing temperature and time. Consequently, AO-80 is a polymorphous material. Study of FT-IR indicated that the intermolecular interactions of several distinct crystals are different. Analysis of the microstructures of crystals by WAXD and FT-IR indicated that the crystal formed by annealing at 100 °C is a smectic crystal, whereas the crystal formed by annealing at 80 °C is a nematic crystal. On the other hand, the AO-80 crystal formed within the CPE matrix during annealing at 100 °C is also a nematic crystal. Though the CPE matrix decreased regularity of AO-80 crystals, it raised the growth rate of the AO-80 crystals.

References

[1] Foldes E. Polym Degrad Stab 1995;49:57.
[2] Wu CF. J Mater Sci Lett 2001;20:1389.
[3] Wu CF. Chin J Polym Sci 2001;19:455.
[4] Wu CF. Nippon Gomu Kyokaishi 2001;74:477.
[5] Wu CF. Chin J Polym Sci 2001;19:455.
[6] Wu CF, Yamagishi T, Nakamoto Y, Ishida S, Nitta K, Kubota S. J Polym Sci, Part B: Polym Phys 2000;38:2285.
[7] Wu CF, Akiyama S. Polym J 2001;33:955.
[8] Wu CF, Nitta K. Kobunshi Ronbunshu 2000;57:449.
[9] Wu CF, Mori K, Otani Y, Namiki N, Emi H. Polymer 2001;42:8289.
[10] Wu CF, Akiyama S, Mabuchi T, Nitta K. Polym J 2001;33:792.
[11] Wu CF, Yamagishi T, Nakamoto Y. Polym Int 2001;50:1095.
[12] Hasui H, Furuhata T, Takanashi K, Omori M. Jpn Patent 1985; 13018.
[13] Foldes E, Turcsanyi B. J Appl Polym Sci 1992;46:507.
[14] Foldes E. J Appl Polym Sci 1994;51:1581.
[15] Foldes E, Lohmeijer J. J Appl Polym Sci 1997;65:761.
[16] Wu CF. J Non-Cryst Solids 2002;315:321.
[17] Pimentel GC, Sederlom CH. J Chem Phys 1956;24:639.